

See discussions, stats, and author profiles for this publication at: <https://www.researchgate.net/publication/347439663>

# Effect of selenium loaded Ribes nigrum nanoparticles on genetic markers in male rats with D-galactose induced toxicity

Article · January 2020

CITATIONS

0

READS

103

2 authors, including:



Masar jabbar Al-kurdy

Al-Furat Al-Awsat Technical University

16 PUBLICATIONS 12 CITATIONS

SEE PROFILE

Some of the authors of this publication are also working on these related projects:



synthesis of selenium nanoparticles [View project](#)

OJVR™

# Online Journal of Veterinary Research®

Volume 24 (5):312-327, 2020.

---

## Effect of selenium loaded *Ribes nigrum* nanoparticles on genetic markers in male rats with D- galactose induced toxicity.

Masar Jabbar Jary Al-Kurdy<sup>1</sup> and Khalisa Khadim Khudair<sup>2</sup>

<sup>1</sup>Nursing, Technical Institute in Al-Diwaniyah, AL-Furat AL-Awsat Technical University, <sup>2</sup>Department of Physiology, biochemistry and Pharmacology, College of Veterinary Medicine, University of Baghdad, Iraq.

### ABSTRACT

Jary Al-Kurdy MJ, Khudair KK., *Effect of selenium loaded Ribes nigrum nanoparticles on genetic markers of male rats with D- galactose induced toxicity, Onl J Vet Res., 24 (5):312-327, 2020.* Authors report effect of selenium nanoparticles loaded with black currant (*Ribes nigrum*) extract on serum caspase3, chromosomes, mitotic index, liver tunnel cells and apoptosis in Wistar male rats given 150mg/kg D-galactose IP daily for 56 days. We generated 18-50nm spherical crystallite nanoparticles identified by UV spectroscopy, electron microscopy and X-ray diffraction. Groups of 8 rats each were then injected 150mg/kg D-galactose IP dissolved in 0.9% saline daily for 8 weeks (Group 1), gavaged 1mg/kg nanoparticles (2) or given both (3). Controls were given saline IP and orally (4). At days 14 and 56, cardiac blood was taken for caspase-3 and femur bone excised for chromosomal aberration and mitotic indices, and livers for DNA fragmentation and apoptosis. Compared with controls, we found significant ( $P < 0.05$ ) declines in serum caspase (~10 to -17%), and chromosomal acentric aberrations (~4 fold) in rats given nanoparticles with or without galactose. In rats given only galactose we found large increases in serum caspase-A (~18%) chromosomal abberations (~12 fold) and mitotic indices (~34%). We found no tunnel liver cells in rats given selenium loaded *Ribes nigrum* nanoparticles with or without D galactose but present throughtout in those given only D-galactose. Results suggest that selenium loaded *Ribes nigrum* nanoparticles nanoparticles may reduce D- galactose genotoxicity in rats and exert anti-oxidants effects.

Key Words: Selenium, nanoparticles, black current, apoptosis, liver.

### INTRODUCTION

Ahmad *et al.*, 2015; Peng *et al.*, 2016; El-Ghazaly *et al.*, 2017; Alagesan and Venugopal, 2019 and Menon *et al.*, (2019) reported that selenium nanoparticles exhibited anti-mutagenic,

antibacterial, anti-inflammatory, anti-microbial and antioxidant activity. Hosnedlova *et al.*, 2018; Khurana *et al.*, (2019) found that oral nanoparticle formulations were well tolerated in patients. Selenium nanoparticles increased cytokines IFN- $\gamma$  and IL-12 in splenocytes of tumor bearing mice and increased delayed hypersensitivity (Sarkar *et al.*, 2015). D-galactose is normally metabolized (Shahroudi *et al.*, 2017) but in excess converts to aldose and hydrogen peroxide by catalysis generating free radicals (Chen *et al.*, 2018). Excess of D-galactose induced aging symptoms of cognitive dysfunction, oxidative stress but decreased antioxidant enzyme activity, immune response and mitochondria (Chang *et al.*, 2016; Jeremy *et al.*, 2017; Sulistyoningrum, 2017; Saleh *et al.*, 2019). We describe effect of selenium nanoparticles loaded with black currant (*Ribes nigrum*) on chromosomes, mitotic index and apoptosis in Wistar male rats gavaged D-galactose daily for 56 days.

## MATERIALS AND METHODS

Black currant aqueous extract was prepared as described by Gottimukkala *et al.*, (2017; Kaikai *et al.*, 2017). Characterization of nanoparticles were evaluated by Ultraviolet–visible spectroscopy (Metertech SP-8001 Taiwan) as described by (Mittal *et al.*, 2013; Banerjee *et al.*, 2014), Fourier-transform infrared spectroscopy (FTIR) (Shimadzu Corporation Japan) (Mittal *et al.*, 2015; Rolim *et al.*, 2019), X-ray diffraction (XRD) (Shemadzu-6000 Japan) (Rietveld, 1969; Holzwarth and Gibson, 2011) and by scanning electron microscopy (SEM-Tescan Vega III, Czech) (Khoshnamvand *et al.*, 2018). After acclimatization for two weeks. thirty-two adult Wistar albino rats (aged 3 months and weighted 200 $\pm$ 10g) were divided randomly and equally into four experimental groups (8/group), each were then injected 150mg/kg D-galactose IP dissolved in 0.9% saline daily for 8 weeks (Group 1), gavaged 1mg/kg nanoparticles (2) or given both (3). Controls were given saline IP and orally (4). Under anesthesia, cardiac blood was taken for serum caspase-3 (Rat CASP3 ELISA kit, Elabscience, USA). At sacrifice (day 56), femur bone marrow was excised to determine chromosomal aberrations as described by Savage, (1976) and mitotic index by Preston *et al.*, (1987). Liver tissue was stained for immunohistochemistry for apoptosis in cells (ApoBrdU-IHC DNA Fragmentation assay kit, Raybio, USA). One and Two-way ANOVA and Least significant differences (LSD) post hoc tests was used to determine significant ( $P < 0.05$ ) differences between means (Snedecor George and Cochran, 1973).

## RESULTS

Results are shown in Figures 1 to 18 and Tables 1 below.

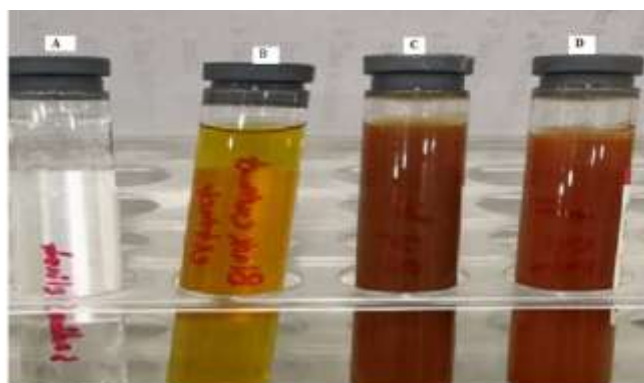


Figure 1. Color reaction between *Ribes nigrum* extract and reduction of sodium selenite nanoparticles. A: sodium selenite, B: Black currant *Ribes nigrum* aqueous extract C: Black currant *Ribes nigrum* loaded selenium nanoparticles by 30min, D: by 48-72 hours.

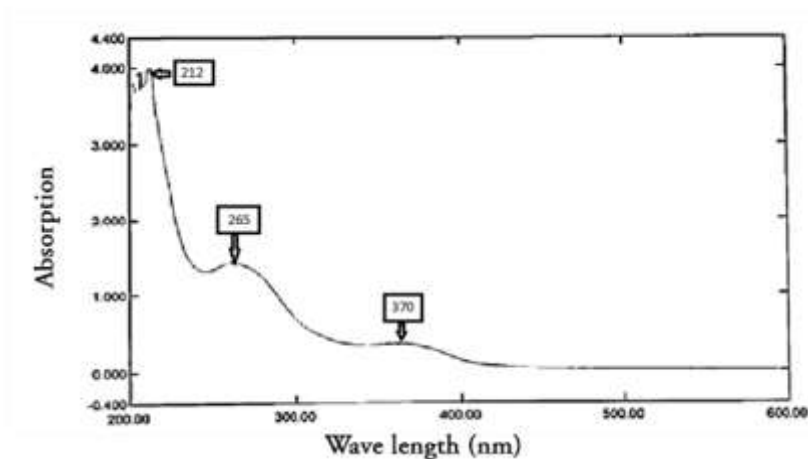


Figure 2: UV-Vis spectra absorbance of selenium loaded *Ribes nigrum* nanoparticles at pH 9.



Figure 3: Electron microscopic image(1 $\mu$ m) of selenium loaded *Ribes nigrum* nanoparticles 1:2 ratio at pH 9

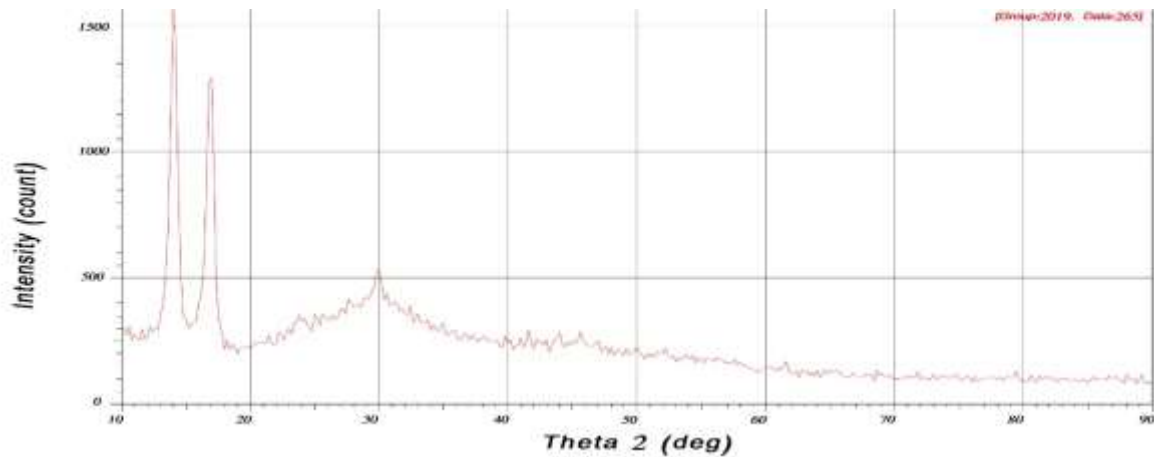


Figure 4. X-ray diffraction curve for selenium loaded *Ribes nigrum* nanoparticles at PH 9

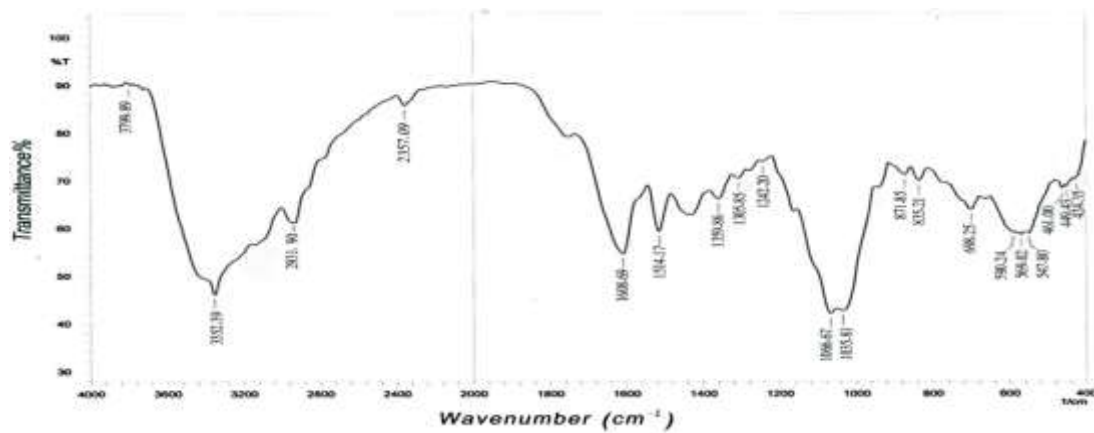


Figure 5. F-TIR spectroscopy of selenium loaded *Ribes nigrum* nanoparticles at PH 9.

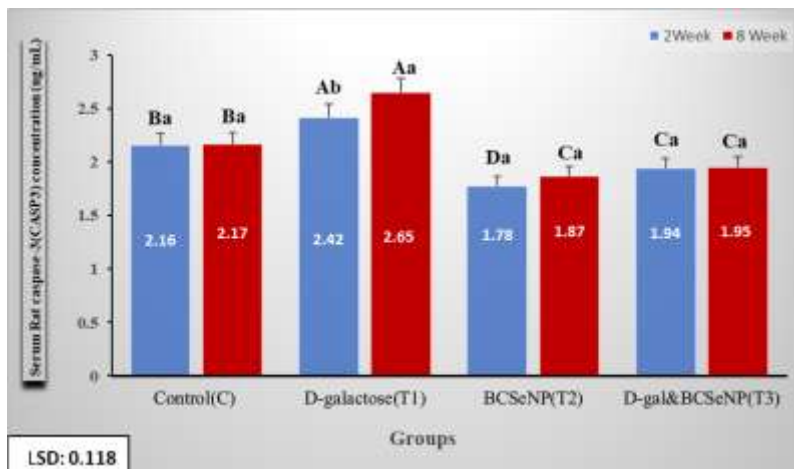


Figure 6. mean  $\pm$  SE serum caspase-3 in rats (n=8) given 150mg/kg daily D galactose (T1) IP with (T3) or without (T2) 1mg/kg nanoparticles and saline controls (C) after 2 and 8 weeks. Different caps were significant between treatments, small letters between periods (P < 0.05).

Table 1 mean  $\pm$  SE chromosomal aberrations (%) in rats (n=8) given 150mg/kg daily D-galactose IP with or without 1mg/kg selenium loaded *Ribes nigrum* nanoparticles and saline controls for 8 weeks.

|                       | Chromosome aberrations % |                      |                     |                      |                          |                      |
|-----------------------|--------------------------|----------------------|---------------------|----------------------|--------------------------|----------------------|
|                       | Fragment                 | . Ring               | Deletion            | Polyploidy           | Acentric                 | Total                |
| Controls              | 0.03 $\pm$ 0.002b        | 0.13 $\pm$ 0.01b     | 0.10 $\pm$ 0.004b   | 0.09 $\pm$ 0.01 b    | 0.14 $\pm$ 0.06a         | 0.51 $\pm$ 0.07b     |
| Galactose             | 0.23 $\pm$ 0.03a 7*      | 2.48 $\pm$ 0.16a 19* | 0.23 $\pm$ 0.01a 2* | 3.10 $\pm$ 0.28a 34* | 0.14 $\pm$ 0.01a         | 6.20 $\pm$ 0.25a 12* |
| Particles             | 0.02 $\pm$ 0.002b        | 0.12 $\pm$ 0.005b    | 0.07 $\pm$ 0.009b   | 0.09 $\pm$ 0.01 b    | 0.03 $\pm$ 0.006b - 4.6* | 0.35 $\pm$ 0.01b     |
| Galactose + particles | 0.02 $\pm$ 0.002 b       | 0.08 $\pm$ 0.01b     | 0.10 $\pm$ 0.005b   | 0.13 $\pm$ 0.01 b    | 0.04 $\pm$ 0.008b - 4.2* | 0.39 $\pm$ 0.03b     |
| LSD <sub>0.05</sub>   | 0.045                    | 0.246                | 0.032               | 0.413                | 0.102                    | 0.391                |

Different letters (P>0.05) between treatments. \*Xfold difference with controls

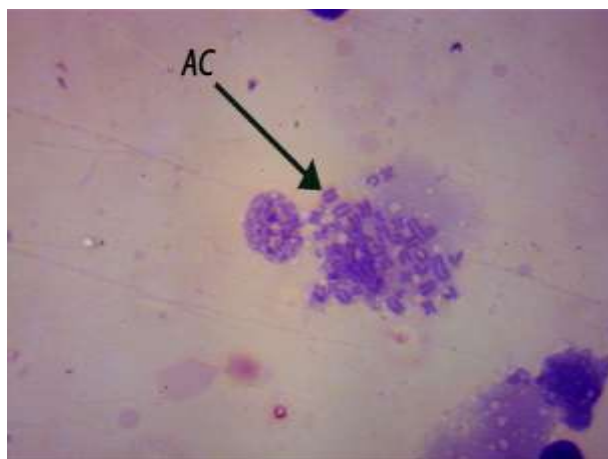


Figure 7: Bone marrow saline controls: Metaphase (AC) normal acentric chromosomes Giemsa stain(1000X)

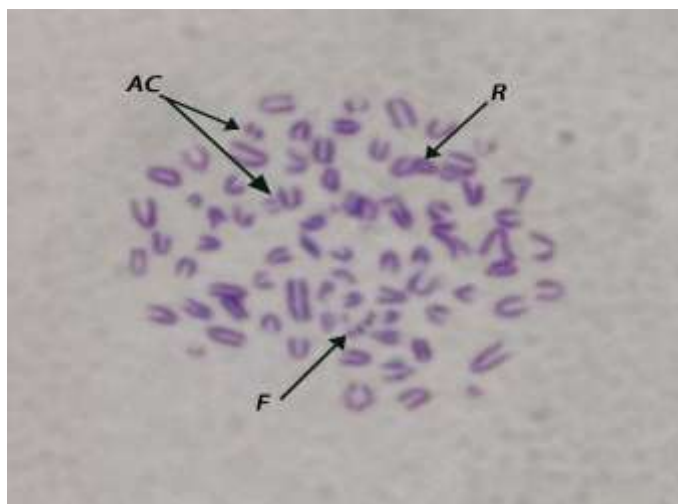


Figure 8. Bone marrow saline controls Metaphase (R) ring, (F) fragment, and (AC) acentric chromosomes. Giemsa stain (1000X).

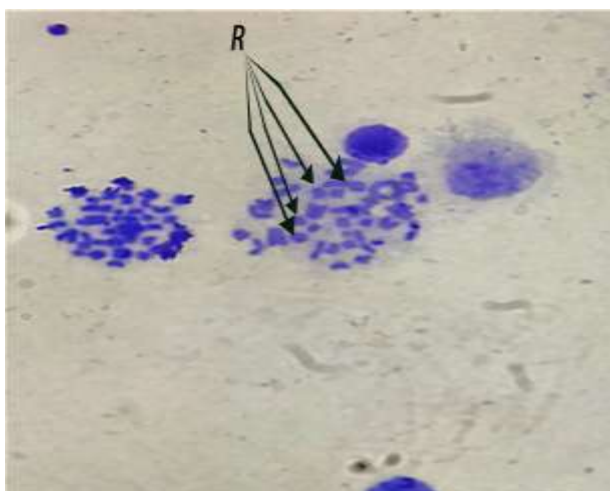


Figure 9. Bone marrow metaphase: rats given 150mg/kg D galactose daily for 56 days (R) ring chromosomes. Giemsa stain (1000X).

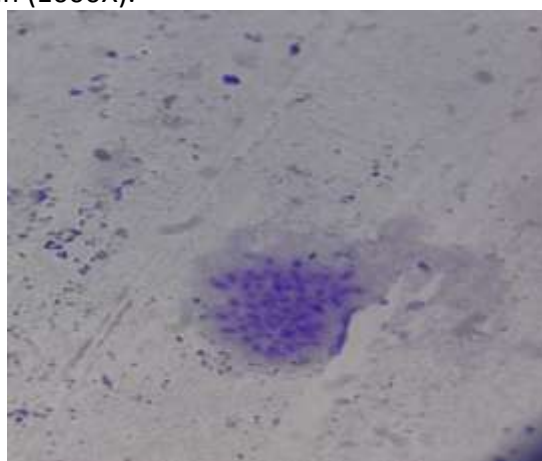


Figure 9. Bone marrow metaphase: rats gavaged 150mg/kg D galactose daily for 56 days showing Polyplody in chromosomes. Giemsa stain(1000X).

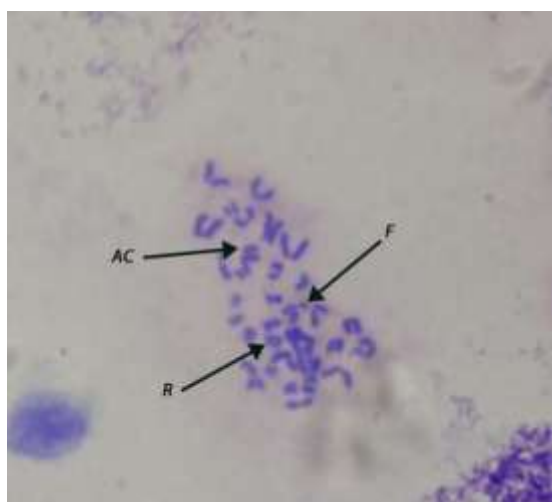


Figure 10. Bone marrow metaphase: rats given 1mg/kg selenium loaded *Ribes nigrum* nanoparticles IP daily for 56 days (F) fragmented, (AC) acentric and, (R) Ring chromosomes. Giemsa stain (1000X).

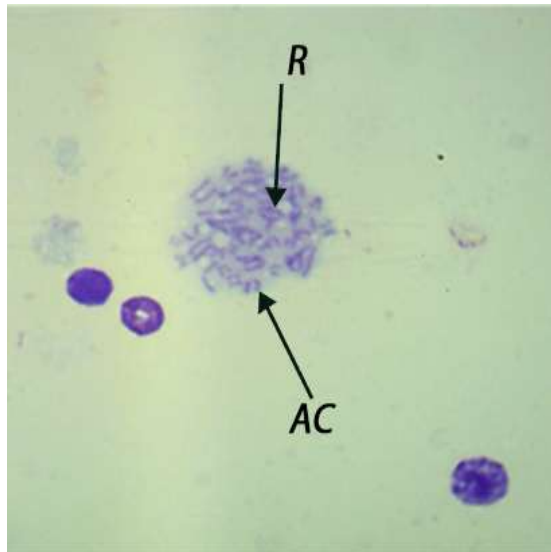


Figure 11. Bone marrow metaphase: rats given 1mg/kg selenium loaded *Ribes nigrum* nanoparticles IP daily for 56 day showing (AC) acentric and (R) Ring chromosomes. Giemsa stain (1000X)

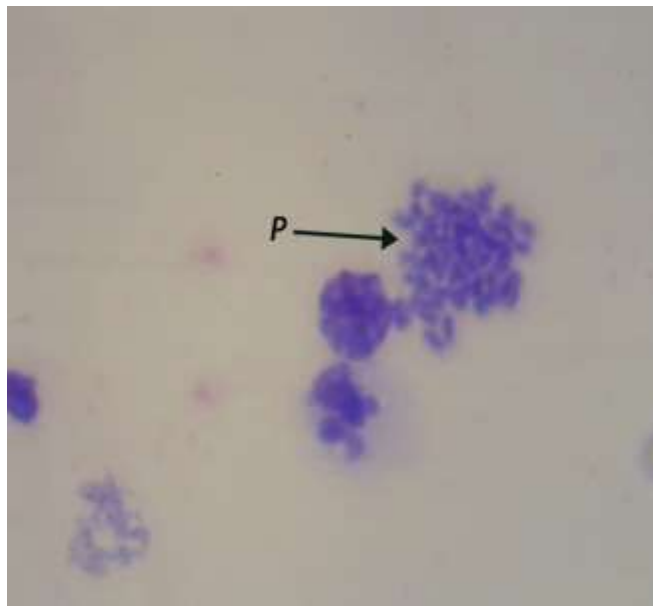


Figure 12. Bone marrow metaphase: rats given 1mg/kg selenium loaded *Ribes nigrum* nanoparticles IP with 150mg/kg D-galactose daily for 56 day showing polyploidy in chromosomes. Giemsa stain (1000X)



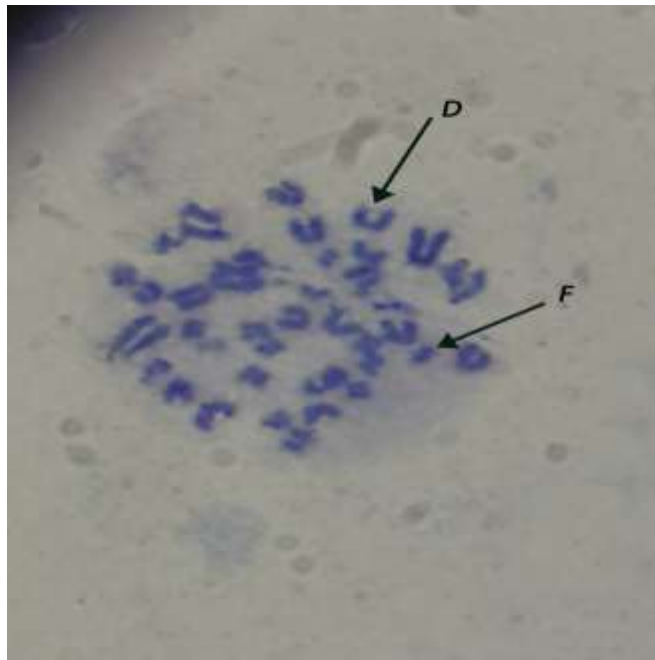


Figure 13. Bone marrow metaphase: rats given 1mg/kg selenium loaded *Ribes nigrum* nanoparticles IP with 150mg/kg gavaged D-galactose daily for 56 days showing (F) fragmentation, (D) deleted and polyploidy in chromosomes. Giemsa stain (1000X)

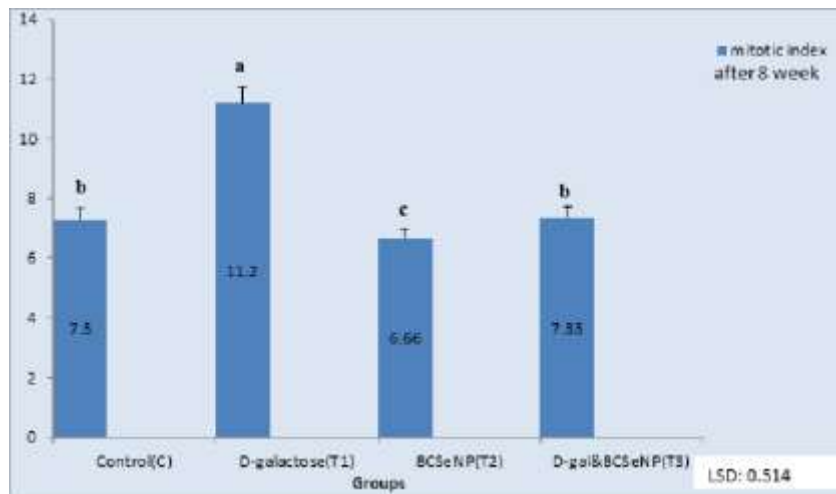


Figure 14: Mean  $\pm$  SE mitotic indices in rats (n=8) given 150mg/kg daily D galactose (T1) IP with (T3) or without (T2) 1mg/kg nanoparticles and saline controls (C) after 2 and 8 weeks. Different letters between treatments ( $P < 0.05$ ).

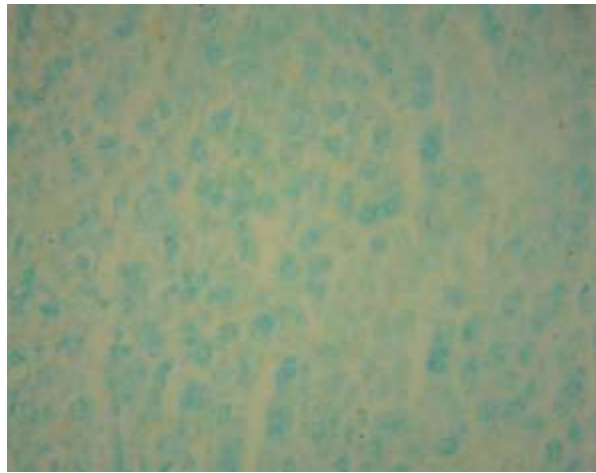


Figure 15. Liver saline controls shows no TUNEL cells determined by ApoBrdU-IHC DNA Fragmentation assay kit (400X).

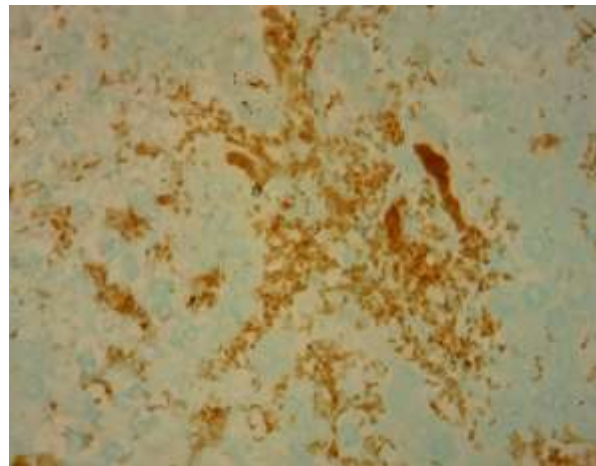


Figure 16. Liver of rats injected 150mg/kg D-galactose daily for 56 days reveals stained TUNEL cells throughout as determined by ApoBrdU-IHC DNA Fragmentation assay kit (400X).



Figure 17. Liver rat injected 1mg/kg selenium loaded *Ribes nigrum* nanoparticles IP daily for 56 days shows no TUNEL cells determined by ApoBrdU-IHC DNA Fragmentation assay kit (400X).



Figure 18. Liver rat injected 1mg/kg selenium loaded *Ribes nigrum* nanoparticles IP with 150mg/kg oral D-galactose daily for 56 days shows no TUNEL cells determined by ApoBrdU-IHC DNA Fragmentation assay kit (400X).

## DISCUSSION

As per previous techniques (Sharma *et al.*, 2014; Gottimukkala *et al.*, 2017; Kaikai *et al.*, 2017) we found that the reduction reaction of *Ribes nigrum extract* with selenium nanoparticles occurred at ~30 minutes when the solution became red and was left to stabilize 48-72 hours as shown in Figure 1. We confirmed nanoparticles by UV-Vis spectroscopy with absorption peaks between (265-370 nm) as shown in Figure 2 (Fesharaki *et al.*, 2010; Zhang *et al.*, 2011; Harikrishnan *et al.*, 2012). Scanning electron microscopy revealed spherical amorphous crystallized nanoparticles with a diameter range of 18-50 nm (Figure 3) (Bunglavan *et al.*, 2014; Riva *et al.*, 2018). X-ray diffraction revealed peaks at theta angle-2 with values of 24.142°, 29.972°, 41.91°, 44.651° and 46.782° corresponded to hkl of (100), (101), (110), (102) and (111)

crystal planes (Figure 4) which corresponds to the reported value (JCPDS File No. 06-362) (Ingole *et al.*, 2010; Sharma *et al.*, 2014; Saratale *et al.*, 2017). Figure (5) showed the F-TIR spectroscopy for selenium nanoparticles. The distinct peak of BCSenNPs was seen at 3352.39 cm<sup>-1</sup> corresponds to OH: NH due to Stretch Vibration in Amide A. While absorption peak at 2931.90 cm<sup>-1</sup> correspond to C-H in -CH<sub>2</sub> in aliphatic compounds. While, the band at 1608.69cm<sup>-1</sup> indicating NH<sub>2</sub> in primary Amides. The peak at 1514.17 cm<sup>-1</sup> is due to NH in secondary Amides (Amide II). The peak at 1359.86 cm<sup>-1</sup> attributed to the C-H bending in alkanes. However, the peaks at 1066.67 and 1035.81 cm<sup>-1</sup> confirm C–O, C–C Stretching Vibrations, C–O–H, C–O–C bending Vibrations in polysaccharides, protein and polyesters. C–X stretching in alkyl halides causes a band at 871.85 and 835.21 cm<sup>-1</sup>. The band at 590.24 and 547.80 cm<sup>-1</sup> were due to C–N–C Bending in Amines (Kamnev *et al.*, 2017; Tugarova *et al.*, 2018; Alagesan and Venugopal, 2019).

Compared with controls, we found significant (P < 0.05) declines in serum caspase (~-10 to -17%) in those given selenium nanoparticles with or without galactose (Figure 6) whereas in rats given only galactose, we found large increases (~18%). Zhu *et al.*, (2016) found that mRNA expression of p53, bax and caspase 3 declined in rats given cisplatin but increased following selenium treatment. Maiyo and Singh (2017) maintained that selenium could inhibit cancer by protecting DNA damage by free radicals and/or apoptosis. Excessive ROS by mitochondria can lead to apoptosis (Chen *et al.*, 2018; park *et al.*, 2019; kello *et al.*, 2020) and activation of caspase-9 which activates caspases-3 and 7 (Kujoth *et al.*, 2005; Du *et al.*, 2019; Zhang *et al.*, 2019). D-galactose could inhibit expression of Bcl-xL an anti-apoptotic protein (Xia *et al.*, 2019). These findings suggest that our selenium nanoparticles loaded with *Ribes nigrum* extract may have exerted anti-oxidant properties.

Compared with data from rats given only D galactose, we found significantly (P < 0.05) less chromosomal (-12-fold) and acentric aberrations (~-4 fold) as well as mitotic indices (~34%) in rats given nanoparticles with or without galactose (Figures 7-13). Microscopy revealed no TUNEL liver cells in rats given nanoparticles with or without D-galactose whereas in those given only galactose, we found TUNEL cells throughout Figures (15-18). Otton *et al.*, (2004) and Attia, (2010) reported that reactive oxygen species (ROS) can lead to apoptosis and chromosomal aberrations (Kubli and Gustafsson, 2012; Hausenloy and Yellon, 2013; Go *et al.*, 2014). Our results suggest that selenium nanoparticles loaded with *Ribes nigrum extract* may reduce D-galactose induced genotoxicity in rats.

## REFERENCES

- Ahmad, M. S.; Yasser, M. M.; Sholkamy, E. N.; Ali, A. M. and Mehanni, M. M. (2015). Anticancer activity of biostabilized selenium nanorods synthesized by *Streptomyces bikiniensis* strain Ess\_ama-1. *International journal of nanomedicine*, 10: 3389-3401.
- Alagesan, V. and Venugopal, S. (2019). Green synthesis of selenium nanoparticle using leaves extract of *withania somnifera* and its biological applications and photocatalytic activities. *Bionanoscience*, 9(1): 105-116.
- Attia, S. M. (2010). Deleterious effects of reactive metabolites. *Oxidative medicine and cellular longevity*, 3(4): 238-253.

- Banerjee, P.; Satapathy, M.; Mukhopahayay, A. and Das, P. (2014). leaf extract mediated green synthesis of silver nanoparticles from widely available indian plants: synthesis, characterization, antimicrobial property and toxicity analysis. *Bioresour. Bioprocess*, 1: 3.
- Bunglavan, S.J.; Garg, A.K.; Dass, R.S. and Shrivastava, S. (2014). Effect of supplementation of different levels of selenium as nanoparticles/sodium selenite on blood biochemical profile and humoral immunity in male Wistar rats. *Vet World*. 7(12):1075-1081.
- Chang, Y.; Chang, H.; Kuo, W.; Lin, H.; Yeh, Y.; Viswanadha, V. P.; Tsai, C.; Chen, R. J.; Chang, H. and Huang, C. (2016). Anti-Apoptotic and Pro-Survival Effect of Alpinate Oxyphyllae Fructus (AOF) in a D-Galactose-Induced Aging Heart. *International Journal of Molecular Sciences*.17:466.
- Chen, P.; Chen, F. and Zhou, B. (2018). Antioxidative, anti- inflammatory and anti- apoptotic effects of ellagic acid in liver and brain of rats treated by D- galactose. *Scientific Reports*, 8(1): 1-10.
- Du, Z. D.; Yu, S.; Qi, Y.; Qu, T. F.; He, L.; Wei, W. *et al.* (2019). NADPH oxidase inhibitor apocynin decreases mitochondrial dysfunction and apoptosis in the ventral cochlear nucleus of D-galactose-induced aging model in rats. *Neurochemistry international*, 124: 31-40.
- El-Ghazaly, M.A.; Fadel, N.; Rashed, E.; El-Batal, A. and Kenawy, S.A. (2017). Anti-inflammatory effect of selenium nanoparticles on the inflammation induced in irradiated rats. *Canadian journal of physiology and pharmacology*, 95(2):101-110.
- Fesharaki, P.; Nazari, P.; Shakibaie, M.; Rezaie, S.; Banoee, M. and Abdollahi, M. (2010). Biosynthesis of selenium nanoparticles using *Klebsiella pneumoniae* and their recovery by a simple sterilization process. *Braz. J. Microbiol.*41:461–466.
- Go, A. S., Mozaffarian, D., Roger, V. L., Benjamin, E. J., Berry, J. D., Blaha, M. J., ... & Fullerton, H. J. (2014). Executive summary: heart disease and stroke statistics—2014 update: a report from the American Heart Association. *Circulation*, 129(3): 399-410.
- Gottimukkala, K.; Harika, R. and Deevika, Z. (2017). Green synthesis of iron nanoparticles using green tea leaves extract. *Nanomedicine Biotherapeutic Discovery*, 7: 1 – 5.
- Harikrishnan, H.; Abdullah, N.; Ponmurugan, K. and Shyam, R. (2012). Microbial synthesis of selenium nanocomposite using *Saccharomyces cerevisiae* and its antimicrobial activity against pathogens causing nosocomial infection. *Chalcogenide Lett.* 9: 509–515.
- Hausenloy, D. J. and Yellon, D. M. (2013). Myocardial ischemia-reperfusion injury: a neglected therapeutic target. *The Journal of clinical investigation*, 123(1): 92-100.
- Holzwarth, U. and Gibson, N. (2011). The scherrer equation versus the Debye-Scherrer equation. *Nat. Nanotechnol.*, 6:534.
- Hosnedlova, B.; Kepinska, M.; Skalickova, S.; Fernandez, C.; Ruttkay-Nedecky, B.; Peng, Q.; Baron, M.; Melcovam, M.; Opatrilova, R.; Zidkova, J.; Bjørklund, G.; Sochor, J. and Kizek, R. (2018). Nano-selenium and its nanomedicine applications: a critical review. *International Journal of Nanomedicine*, 13: 2107–2128.
- Ingole, A.; Thakare, S.; Khati, N.; Wankhade, A. and Burghate, D. (2010). Green synthesis of selenium nanoparticles under ambient condition. *chalcogenide Lett.* 7:485-489.
- Jeremy, M.; Gurusubramanian, G. and Roy, V. K. (2017). Localization pattern of visfatin (NAMPT) in d-galactose induced aged rat testis. *Annals of Anatomy-Anatomischer Anzeiger*, 211: 46-54.
- Kaikai, B.; Bihong, H.; Jianlin, H.; Zhuan, H. and Ran, T. (2017). Preparation and antioxidant properties of selenium nanoparticles-loaded chitosan microspheres *International Journal of Nanomedicine*, 12: 4527–4539.
- Kamnev, A.A.; Mamchenkova, P.V.; Dyatlova, Y.A. and Tugarova, A.V. (2017). FTIR spectroscopic studies of selenite reduction by cells of the rhizobacterium *Azospirillum brasilense* Sp7 and the formation of selenium nanoparticles. *J Mol Struct.* 1140: 106-112.
- Kello, M.; Takac, P.; Kubatka, P.; Kuruc, T.; Petrova, K. and Mojzis, J. (2020). Oxidative Stress-Induced DNA Damage and Apoptosis in Clove Buds-Treated MCF-7 Cells. *Biomolecules*, 10(1): 139.

- Khoshnamvand, M.; Huo, C. and Liu, J. (2018). Silver nanoparticles synthesis using *Allium ampeloprasum* L. leaf extract: characterization and performance in catalytic reduction of 4-nitrophenol and antioxidant activity. *J. Mol. Struct.*, 1175:90-96.
- Khurana, A.; Tekula, S.; Saifi, M. A.; Venkatesh, P. and Godugu, C. (2019). Therapeutic applications of selenium nanoparticles. *Biomedicine & Pharmacotherapy*, 111: 802–812.
- Kubli, D. A. and Gustafsson, A. B. (2012). Mitochondria and mitophagy: the yin and yang of cell death control. *Circulation research*, 111(9):1208-1221.
- Kujoth, G. C.; Hiona, A.; Pugh, T. D.; Someya, S.; Panzer, K.; Wohlgemuth, S. E.; Hofer, T.; Seo, A.Y.; Sullivan, R.; Jobling, W.A. and Morrow, J.D. (2005). Mitochondrial DNA mutations, oxidative stress, and apoptosis in mammalian aging. *Science*, 309(5733): 481-484.
- Maiyo F. and Singh, M. (2017). Selenium nanoparticles: potential in cancer gene and drug delivery. *Nanomedicine (Lond)* 12:1075–89.
- Menon, S.; KS, S. D.; Agarwal, H. and Shanmugam, V. K. (2019). Efficacy of Biogenic Selenium Nanoparticles from an extract of ginger towards evaluation on anti-microbial and anti-oxidant activities. *Colloid and Interface Science Communications*, 29:1-8.
- Mittal, A. K.; Chaisti, Y. and Banerjee, U. C. (2013). Synthesis of metallic nanoparticles using plant extracts. *Biotechnol. Adv.*, 31:346-356.
- Mittal, A. K.; Tripathy, D.; Choudhary, A.; Aili, P. K.; Chatterjee, A.; Singh, I. P. and Banerjee, U. C. (2015). Bio-synthesis of silver nanoparticles using *Potentilla fulgens* Wall. ex Hook. and its therapeutic evaluation as anticancer and antimicrobial agent. *Materials Science and Engineering: C*, 53: 120-127.
- Otton, R.; Soriano, F. G.; Verlengia, R. and Curi, R. (2004). Diabetes induces apoptosis in lymphocytes. *Journal of Endocrinology*, 182(1): 145-156.
- Park, C.C; hoi, E. O.; Kim, G. Y.; Hwang, H. J.; Kim, B. W.; Yoo, Y. H.; park, T.H. and Choi, Y. H. (2019). Protective effect of Baicalein on oxidative stress-induced DNA damage and apoptosis in RT4-D6P2T Schwann cells. *International journal of medical sciences*, 16(1): 8.
- Peng, F.; Guo, X.; Li, Z.; Li, C.; Wang, C.; Lv, W.; Wang, J.; Xiao, F.; Kamal, M.A. and Yuan, C. (2016). Antimutagenic effects of selenium-enriched polysaccharides from *pyracantha fortuneana* through suppression of cytochrome P450 1A subfamily in the mouse liver. *Molecules*, 21: 1.
- Preston, R. J.; Dean, B. J.; Galloway, S.; Holden, H.; McFee, A. F. and Shelby, M. (1987). Mammalian in vivo cytogenetic assays analysis of chromosome aberrations in bone marrow cells. *Mutation Research/Genetic Toxicology*, 189(2): 157-165.
- Rietveld, H. (1969). A profile refinement method for nuclear and magnetic structures. *J. Appl. Crystallogr.*, 2:65-71.
- Riva, B.; Bellini, M.; Corvi, E.; Verderio, P.; Rozek, E.; Colzani, B., *et al.* (2018). Impact of the strategy adopted for drug loading in nonporous silica nanoparticles on the drug release and cytotoxic activity. *J Colloid Interface Sci.* 519:18-26.
- Rolim, W. R.; Pelegrino, M. T.; de Araújo Lima, B.; Ferraz, L. S.; Costa, F. N.; Bernardes, J. S.; Rodrigues, T.; Brocchi, M. and Seabra, A. B. (2019). Green tea extract mediated biogenic synthesis of silver nanoparticles: Characterization, cytotoxicity evaluation and antibacterial activity. *Applied Surface Science*, 463: 66-74.
- Saleh, D.O.; Mansour, D.F.; Hashad, I.M. and Bakeer, R.M. (2019). Effects of sulforaphane on D-galactose-induced liver aging in rats: role of keap-1/nrf-2 pathway. *Eur J Pharmacol*, 855:40–49.
- Saratale, R.G.; Benelli, G.; Kumar, G.; Kim, D.S. (2017). Saratale GD. Bio-fabrication of silver Nanoparticles using the leaf extract of an ancient herbal medicine, dandelion (*Taraxacum officinale*), evaluation of their antioxidant, anticancer potential, and antimicrobial activity against phytopathogens. *Environ Sci Pollut Res.*25(11):10392–10406.
- Sarkar, B.; Bhattacharjee, S.; Daware, A.; Tribedi, P.; Krishnani, K. K. and Minhas, P. S. (2015). Selenium nanoparticles for stress-resilient fish and livestock. *Nanoscale research letters*, 10(1): 371.

- Savage, J. R. (1976). Classification and relationships of induced chromosomal structural changes. *Journal of medical genetics*, 13(2): 103-122.
- Shahroudi, M. J.; Mehri, S. and Hosseinzadeh, H. (2017). Anti-aging effect of *Nigella sativa* fixed oil on D-galactose-induced aging in mice. *Journal of pharmacopuncture*, 20(1): 29.
- Sharma, G.; Sharma, A.R.; Bhavesh, R.; Park, J.; Ganbold, B.; Nam, J.S. *et al.* (2014). Biomolecule-mediated synthesis of selenium nanoparticles using dried *Vitis vinifera* (raisin) extract. *Molecules*.19:2761–70.
- Snedecor George, W. and Cochran, W. G. (1973). *Statistical methods*. Iowa State University Press.
- Sulistyoningrum, E. (2017). D-galactose-induced animal model of male reproductive aging. *Jurnal Kedokteran dan Kesehatan Indonesia*, 8(1): 19-28.
- Tugarova, A.V.; Mamchenkova, P.V.; Dyatlova, Y.A. and Kamnev, A.A. (2018). FTIR and Raman spectroscopic studies of selenium nanoparticles synthesised by the bacterium *Azospirillum thiophilum*. *Spectrochim Acta A Mol Biomol Spectrosc.* 192: 458-463.
- Xia, Y.; Zhong, J.; Zhao, M.; Tang, Y.; Han, N.; Hua, L.; Xu, T.; Wang, C. and Zhu, B. (2019). Galactose-modified selenium nanoparticles for targeted delivery of doxorubicin to hepatocellular carcinoma. *Drug Delivery*, 26(1):1-11.
- Zhang, W.; Chen, Z.; Liu, H.; Zhang, L.; Gao, P. and Li, D. (2011). Biosynthesis and structural characteristics of selenium nanoparticles by *Pseudomonas alcaliphila*. *Colloids Surf B.* 88:196–202.
- Zhang, Z.; Tian, L. and Jiang, K. (2019). Propofol attenuates inflammatory response and apoptosis to protect d-galactosamine/lipopolysaccharide induced acute liver injury via regulating TLR4/NF- $\kappa$ B/NLRP3 pathway. *International immunopharmacology*, 77: 105974.
- Zhu, K.; Jiang, L.; Chu, Y. and Zhang, Y. S. (2016). Protective effect of selenium against cisplatin-induced nasopharyngeal cancer in male albino rats. *Oncology letters*, 12(6): 5068-5074.